

# A numerical analysis of heat transfer inside internal combustion engines

Khong Vu Quang<sup>a</sup>, Vu Minh Dien<sup>a, b</sup>, Nguyen Duy Tien<sup>a</sup>, Nguyen The Luong<sup>a</sup>, Pham Minh Tuan<sup>a</sup>

<sup>a</sup>School of Transportation Engineering, Hanoi University of Science and Technology, Vietnam

<sup>b</sup>Faculty of Automotive Technology, Hanoi University of Industry, Vietnam

**Abstract**—Utilizing the regenerative heat from the exhaust gases and the coolant water to generate useful power is a potential solution to improve the efficiency of the internal combustion engine (ICE). The recovery efficiency significantly depends on the actual waste heat energy in specific operating conditions of ICE. This article presents a study on a simulating model to calculate the amount of waste heat flow out of the exhaust gases and the coolant water of an ICE by 1D simulation software, named AVL-Boost. The results show that the heat transfers to the exhaust gases and the coolant water that could generate much more useful power is approximately 60-70%, and reaches a maximum value at the full load condition. Based on these results, the heat energy recovery system could be calculated, designed and optimized to utilize the exhaust gases and coolant water of ICE within difference conditions.

**Index Terms**—Internal combustion engine, heat and transfer, engine performance, regenerative heat, fuel consumption.

## I. INTRODUCTION

In recent years, thermal efficiency has been considered as an important criterion to evaluate the operating characteristics of internal combustion engines (ICE). To achieve this criterion, many technical solutions have been applied by the ICE manufacturing industry and achieved goals with the thermal efficiency of approximately 30-40%. However, there is still a large amount of heat energy loss emitting to the environment, corresponding to 60-70% of total energy [1-3]. Moreover, the needs for using fossil fuel are increasing; reserves being exhausted; the price is dancing and has an increasing tendency; energy security contains many latent risks; while the requirement for ICE emissions has been tightened [4-9]. As a result, the ICE manufacturing industry always demands better thermal efficiency and emissions reduction. Therefore, many eco-friendly technologies have been deployed in worldwide applications. One of the potential solution to improve thermal efficiency is recovering heat energy from exhaust gases and coolant water of ICE that has been studied by many researchers in this field. For example, M. Hatami et al. performed some research to reach the optimal structure for the ICE exhaust gases utilizer tube to produce useful power [10]. M. Ghazikhani et al. evaluated the effectiveness of utilizing exhaust energy to produce useful power when ICE working in different loads and speed which result shows fuel consumption rate could be reducing by up to 10% [11]. E.H Wang et al. revealed and specified some organic liquid for the Rankine cycle to improve the efficiency of utilizing waste heat from exhaust gases in ICE [12].

V. Pandiyarajan et al. researched on utilizing waste heat of diesel engine by the combined system of exchange and store thermal power, the result shows that 10 to 15% of fuel energy conservation could be utilized in the form of thermal energy by the thermal storage device [13]. R. Saidur et al. performed some research and evaluation of new technology solutions of utilizing exhaust energy to produce useful power. The fields they studied are: using the hybrid engine, the steam turbine in the ORC cycle and turbo charge by compressor turbine. The research results indicate that the utilizing waste heat of ICE will contribute to improve fuel efficiency, reduce the needs to use fossil fuel and help slow down global warming [14]. A. Boretti had researched on utilizing waste heat from exhaust gases and coolant water to produce useful power which operates in the ORC cycle on a hybrid car. The result shows engine efficiency can be improved up to 8.2% [1]. S. Bari et al. performed some research on utilizing exhaust gases from a diesel engine with water as a solvent and go through a system with 2 heat exchanger. After the system had been optimized, the outcome was excellent with the engine power increased by 16% to 23.7% [15]. F. Jian-qin et al. had studied on utilizing waste heat from engine's coolant by the ORC cycle using low temperature, the result shows fuel consumption efficiency can be improved up to 12.1% [16]. T. Y. Kim et al. had performed some field experiment to evaluate the effects of engine regime to the feature of the hybrid engine utilizing waste heat from exhaust gases. The results show that the characteristic of the hybrid engine depends on loads and speed of the engine and power efficiency can be improved by 2.8% [17]. Q. Cao et al. had researched to improve the efficiency of the hybrid engine when utilized waste heat from exhaust gases. The result indicated that with the most optimize exchanged heat tube could push the efficiency by 2.58% [18]. M. E. Demir et al. had researched and developed a waste heat utilizing system on hybrid engines. The outstanding outcome shows that engines power can be improved to 90% [19]. In another research, T.ae Y. Kim et al. studied the effects of different engine regime to the ability of utilizing waste heat from exhaust gases on hybrid engines. The result indicated waste heat utilizing efficiency can achieve 5.7 to 11.1% [20].

However, these solutions still not exploit the most energy of the waste heat. The previously calculated results are only exact at a stable engine regime with a large amount of exhaust gases. While in the real situation, ICE always works at variable loads and speed leading to the change of the amount of waste heat which affects the heat utilizing the efficiency of the system. Thus, to maximize the efficiency and the basis to design the systems that can achieve high efficiency in

Manuscript received: 24 September 2018

Manuscript received in revised form: 22 October 2018

Manuscript accepted: 05 November 2018

Manuscript Available online: 10 November 2018

different engine regime this study had conducted the research focusing on developing an intelligent simulation model. That calculates the amount of heat loss to coolant and exhaust gases by the simulation program AVL-boost.

The results show that in full load and rated speed  $q_{Cool}$  is about 26% and reduces gradually as the speed down;  $q_{Exh}$  is about 32.5% while  $q_{Otherloss}$  accounts for about 10% and they tend to decrease directly proportional to speed. The study results would be the significant basis to calculate, design and implement the system utilizing the heat energy transferred to cooling water and exhaust gas of the ICE.

## II. TEST ENGINE SIMULATION PROCEDURES

### A. The method and test engine characteristics

The research is performed on AVL-Boost software, where the set of configuration and calibration parameters of the model are based on the specifications of engine and experiment on the test bed. Run the simulation model in the load modes changed from 30% to 100% with the step of 10% and the speed range from 1000 rpm to 2200 rpm with the step of 200 rpm. The D243 diesel engine has been selected as the object of this research, which is a diesel engine used in many different transportation vehicles such as road vehicles, river ships, agricultural machines in Vietnam. The specifications of the engine are shown in Table 1.

Table 1. The specifications of D243 engine

Order	Parameter	Value
1	Type of engine	Diesel, 4 stroke
2	Volume	4.75 L
3	Bore x stroke	110mm x 125mm
4	Compression ratio	16.7
5	Length of connecting rod	230 mm
6	Rated speed	2200 rpm
7	Rated power	56 kW/2200 rpm
8	Rated torque	740 Nm/1400 rpm

### B. Basic conservation equations

The simulation model of this engine was built by the AVL-Boost program. The elements of the model were selected base on the specifications of the researched engine. The computation of the simulation model is implemented by the combination between the first law of thermodynamics with the calculation models of combustion, heat transfer and gas exchange [21].

#### 1. The first law of thermodynamics equation

The expansion of the ICE is an irreversible process that converts chemical energy into thermal energy. The determination of the state of the mixture at each point in the process requires a detailed understanding of the intermediate chemical reactions that change from the original mixture to the final combustion products. But this is a difficult and complex problem. However, using the first law of thermodynamics can determine the relationship between the beginning stage and the finish stage of that process without

regarding the intermediate stages [21]. Apply the first law to calculate the combustion process in engine gets equation (1).

$$\frac{d(m_c \cdot u)}{d\alpha} = -p_c \frac{dV}{d\alpha} + \frac{dQ_F}{d\alpha} - \sum \frac{dQ_w}{d\alpha} - h_{BB} \frac{dm_{BB}}{d\alpha} \quad (1)$$

Where,  $\frac{d(m_c \cdot u)}{d\alpha}$  is the change of the internal energy in the cylinder;  $-p_c \frac{dV}{d\alpha}$  in the piston work;  $\frac{dQ_F}{d\alpha}$  in the fuel heat input;  $\sum \frac{dQ_w}{d\alpha}$  is the wall heat losses;  $h_{BB} \frac{dm_{BB}}{d\alpha}$  is the enthalpy flow due to blow-by;  $\frac{dm_{BB}}{d\alpha}$  is the blow-by mass flow;  $\alpha$  is the crank angle;  $h_{BB}$  is the enthalpy of blow-by;  $m_c$  is the mass of mixture in cylinder;  $u$  is the specific internal energy;  $p_c$  is the cylinder pressure;  $V$  is the cylinder volume;  $Q_F$  is the fuel energy;  $Q_w$  is the wall heat loss. With the assumptions: the fuel added to the cylinder charge is immediately combusted; combustion mixture is immediately blended with the residual gas in the cylinder; A/F ratio decreases continuously from a high value at the start to a low value at the end of the expansion process. And after performing equation (1), there have equation (2) to determine the temperature variation in the cylinder depending on the crank angle:

$$\frac{dT_c}{d\alpha} = \frac{1}{m_c \left( \frac{\partial u}{\partial T} + \frac{\partial u}{\partial p} \cdot \frac{p_c}{T_c} \right)} \left[ \frac{dQ_F}{d\alpha} \left( 1 - \frac{u_c + \frac{\partial u}{\partial p} p_c}{H_u} \right) - \frac{dQ_w}{d\alpha} - \frac{dm_{BB}}{d\alpha} \left( h_{BB} - u_c - p_c \frac{\partial u}{\partial p} \right) - m_c \frac{\partial u}{\partial \lambda} \frac{\partial \lambda}{\partial \alpha} - p_c \frac{dV_c}{d\alpha} \left( 1 - \frac{\partial u}{\partial p} \frac{m_c}{V_c} \right) \right] \quad (2)$$

Where,  $T_c$  is the temperature of the mixture in the cylinder;  $u_c$  is the specific internal energy of mixture in the cylinder;  $H_u$  is the low calorific value of fuel;  $\lambda$  is the equivalence ratio.

The solution of equation (2) depends on the combustion model, the rule of heat generation and the heat transfer through the cylinder wall, as well as the pressure, temperature and properties of the gas mixture. After using the Runge-kutta method for determining the solution of equation (2), the temperature in the cylinder is identified. Then they are combined with equation (3) to determine the pressure in the cylinder ( $p_c$ ).

$$p_c = \frac{1}{V} \cdot m_c \cdot R_c \cdot T_c \quad (3)$$

Where,  $R_c$  is the gas constant for the mixture in the cylinder.

#### 2. The combustion model

AVL\_MCC combustion model is selected because it is suitable for the direct injection diesel engine. This model can predict combustion parameters including the rate of waste heat energy and combustion products depending on the

amount and rule of fuel supply. The model also considers the effects of premixed (PMC) and mixing-controlled (MCC) combustion processes and it is calculated by equation (4).

$$\frac{dQ_{\Sigma}}{d\alpha} = \frac{dQ_{MCC}}{d\alpha} + \frac{dQ_{PMC}}{d\alpha} \quad (4)$$

Using equation (5) for the MCC phase, while the PMC is determined by equation (8).

$$\frac{dQ_{MCC}}{d\alpha} = C_{comb} \cdot f_1(m_F, Q_{MCC}) \cdot f_2(k, V) \quad (5)$$

$$\text{with } f_1(m_F, Q_{MCC}) = m_F - \frac{Q_{MCC}}{H_u} \quad (6)$$

$$\text{and } f_2(k, V) = \exp\left(C_R \cdot \frac{\sqrt{k}}{\sqrt[3]{V}}\right) \quad (7)$$

$$\frac{dQ_{PMC}}{d\alpha} = \frac{Q_{PMC}}{\Delta\alpha_c} = \frac{a}{\Delta\alpha_c} \cdot (m+1) \cdot y^m \cdot e^{-a \cdot y^{m+1}} \quad (8)$$

Where,  $C_{comb}$  is the constant of the model;  $Q_{MCC}$  is the cumulative heat release for the mixture controlled combustion;  $Q_{PMC}$  is the total fuel heat input for the premixed combustion;  $m_F$  is the mass of fuel injection;  $C_R$  is a mixing rate constant;  $k$  is the local density of turbulent kinetic energy;  $V$  is cylinder volume.

### 3. The heat transfer model

The heat transferred from the combustion chamber to the cooling water through the walls of the combustion chamber, such as the cylinder head, piston and liner, is determined by equation (9) [23].

$$Q_{wi} = A_i \alpha_w (T_c - T_{wi}) \quad (9)$$

Where,  $Q_{wi}$  is the wall heat flow (cylinder head, piston, liner);  $A_i$  is the surface area (cylinder head, piston, liner);  $\alpha_w$  is the heat transfer coefficient;  $T_c$  is the gas temperature in the cylinder;  $T_{wi}$  is the wall temperature (cylinder head, piston, liner).

There are many models to determine the heat transfer coefficient in AVL-Boost, but the Woschni 1978 model is suitable for the D243 engine with the toroidal chamber and the heat transfer coefficient is summarized as follows, equation (10) [22].

$$\alpha_w = 130 p_c^{0.8} D^{-0.2} T_c^{-0.53} \left[ C_1 c_m + C_2 V_h T_{cl} \frac{p_c - p_{ck}}{p_{cl} V_{cl}} \right]^{0.8} \quad (10)$$

Where,  $p_{ck}$  is the cylinder pressure of the motored engine;  $D$  is the cylinder bore;  $c_m$  is the mean piston speed;  $V_h$  is the displacement per cylinder;  $p_{cl}$ ,  $T_{cl}$ ,  $V_{cl}$  are the pressure, temperature and volume in the cylinder at intake valve closing (IVC).

In addition, for the direct injection diesel engine, the coefficients  $C_1$  and  $C_2$  are calculated as follows:

$C_1 = 6.18 + 0.417 (c_u/c_m)$  for the gas exchange process, while other processes  $C_1 = 2.28 + 0.308 (c_u/c_m)$  with  $c_u$  is the circumferential velocity and calculated by formula

$c_u = \pi \cdot D \cdot n_d / 60$ ,  $n_d$  is the swirl velocity of gas in cylinder and  $n_d = 8.5 \cdot n$  ( $n$  is the rotational speed of crankshaft in rpm);

$C_2 = 3.24 \cdot 10^{-3}$  when combustion occurs and  $C_2 = 0$  in others processes.

During overlap period, it is also very important to consider the heat transfer in the intake and exhaust ports because the gas throttles through slot narrow at valves and valve seats with the high heat transfer coefficients and temperatures. In the AVL-Boost, the Zapf model [21] is used to calculate.

$$T_d = (T_u - T_w) \cdot e^{\left(-A_w \frac{\alpha_p}{\dot{m} \cdot c_p}\right)} + T_w \quad (11)$$

The heat transfer coefficient  $\alpha_p$  depends on the direction of the flow (in or out of the cylinder). For inflow uses equation (12) and outflow uses equation (13):

$$\alpha_p = [C_4 + C_5 \cdot T_u - C_6 \cdot T_u^2] \cdot T_u^{0.44} \cdot \dot{m}^{0.5} \cdot d_{vi}^{-1.5} \cdot \left[1 - 0.797 \cdot \frac{h_v}{d_{vi}}\right] \quad (12)$$

$$\alpha_p = [C_7 + C_8 \cdot T_u - C_9 \cdot T_u^2] \cdot T_u^{0.33} \cdot \dot{m}^{0.68} \cdot d_{vi}^{-1.68} \cdot \left[1 - 0.765 \cdot \frac{h_v}{d_{vi}}\right] \quad (13)$$

Where,  $\alpha_p$  is the heat transfer coefficient in the port;  $T_d$  is the downstream temperature;  $T_u$  is the upstream temperature;  $T_w$  is the port wall temperature;  $A_w$  is the port surface area;  $\dot{m}$  is the mass flow rate;  $c_p$  is specific heat at constant pressure;  $h_v$  is the valve lift of intake or exhaust valve;  $d_{vi}$  is the inner valve seat diameter. Other constant factors, using in above formulas, are shown in Table 2.

**Table 2. Constant values of the heat transfer equation at intake and exhaust valves**

Exhaust valve		Intake valve	
$C_4$	1.2809	$C_7$	1.5132
$C_5$	$7.0451 \cdot 10^{-4}$	$C_8$	$7.1625 \cdot 10^{-4}$
$C_6$	$4.8035 \cdot 10^{-7}$	$C_9$	$5.3719 \cdot 10^{-7}$

## III. TEST ENGINE SIMULATION IN AVL-BOOST SOFTWARE

### A. Building the test engine model

Based on the D243 engine structure, measurement parameters and documents related, the elements of the simulation model are selected appropriately and shown in Figure 1. Type and number of elements are shown in Table 3. The general data of model and the major parameters of elements are shown in Table 4.

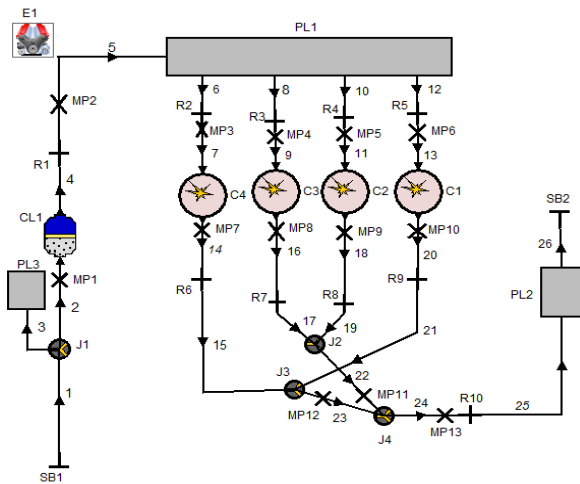


Fig.1: Simulation model of D243 engine in AVL-Boost

Table 3. Elements of D243 engine simulation Model on AVL-Boost

	Name	Value
1	System Boundary	2
2	Air Cleaner	1
3	Engine	1
4	Cylinder	4
5	Pipe	26
6	Measuring point	13
7	Junction	4
8	Restriction	10
9	Plenum	3

Table 4: The general parameters of D243 engine model on AVL-Boost

	Name	Value	Unit
1	Engine type	4 Stroke	-
2	Firing order	1-3-4-2	-
3	Pressure of environment	1	bar
4	Temperature of environment	25	°C
5	Low calorific value of fuel $Q_H$	42800	kJ/kg
6	A/F	14.7	-
7	Combustion model	AVL MCC	-
8	Number of injection holes	5	-
9	Hole diameter	0.3	mm
10	Injection pressure	180	bar
11	Start of injection	24	CA

**B. Verification and validation of the simulation model**

**1. Experimental procedure**

The power and fuel consumption of the engine at the maximum of the fuel adjustment position are determined as the basic inputs for building, correction and assessment of the reliability of model of the D243 engine by AVL-Boost. To specify these parameters, the D243 engine was tested and

measured on the engine test bed, as shown in Figure.2. The experiment was conducted at the Internal Combustion Engine Laboratory, Hanoi University of Science and Technology.

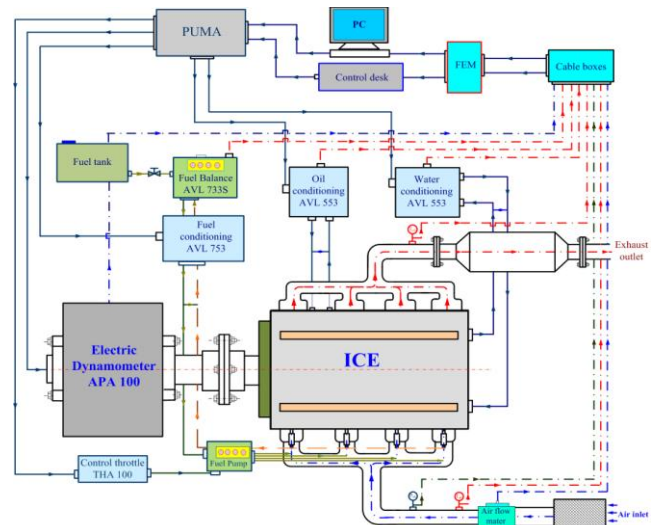


Fig.2: Schematic arrangement of engine testbed

The testbed consists of the following main devices: AVL APA 100 dynamometer, Oil cooler AVL 554, Coolant system AVL 553, AVL fuel balance 733S, Fuel temperature control AVL 753, Throttle actuator THA 100 and PUMA software.

**2. Calibration and evaluation of the proposed model**

After inserting the data into the simulation model, the process of running and modifying model was completed base on the experimenting results. This process only stops when the simulation results narrow the gaps with experiment results. Then continue running the model at the points of maximum fuel mass injection to compare between the simulation (Si) and the experiment results (Ex). The reliability of the model is evaluated by the difference between the power and fuel consumption of the Si and Ex, the results are shown in Table 5 Figure 3.

Table 5: Compared the  $N_e$  and  $g_e$  between simulation (Si) and experiment (Ex) of D243 engine

Order	n (rpm)	$N_e$ (kW)		Deviation (%)	$g_e$ (g/kW.h)		Deviation (%)
		Ex	Si		Ex	Si	
1	1000	26.68	27.98	4.87	281.26	268.19	-4.65
2	1200	32.10	33.38	3.99	274.49	263.98	-3.83
3	1400	40.65	41.98	3.27	270.77	262.17	-3.18
4	1600	47.11	48.26	2.44	269.28	261.86	-2.76
5	1800	49.56	50.12	1.13	267.14	261.39	-2.15
6	2000	50.35	51.74	2.76	268.21	262.08	-2.28
7	2200	54.08	54.56	0.89	272.51	265.86	-2.44

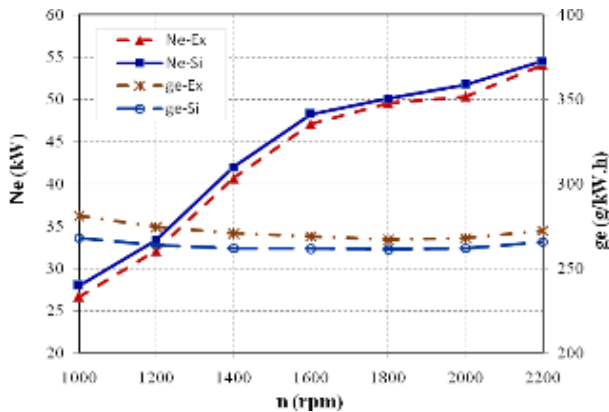


Fig 3:  $N_e$  and  $g_e$  of Si and Ex models

The results in Table 5 and Fig. 3 indicate that the values of  $N_e$  and  $g_e$  between Si and Ex to be very close. All of the deviations are less than 5%, in which the greatest error of  $N_e$  is 4.87% and  $g_e$  is 4.65% at  $n = 1000$  rpm. These deviations due to the assumptions in the simulation model that is improper compared with the experimental conditions. However, these errors are small and accepted which mean that this model is usable and reliable. Therefore, it is possible using the D243 engine model to perform further simulation modes.

#### IV. RESULTS AND DISCUSSION

With the reliability model as mention above, the D243 engine model on AVL-Boost was used to simulate in steady states at baseline map in ranges of 30% to 100% load, at the speed of 1000 rpm to 2200 rpm, the step-by-step implementation of 10% for load and 200 rpm for speed. The parameters of the engine are identified, including:  $N_e$  and  $g_e$ ; Ratio of heat transfer to useful work ( $q_e$ ); The amount and rate of energy losses to the coolant system ( $Q_{Cool}$ ,  $q_{Cool}$ ), to exhaust gas ( $Q_{Exh}$ ,  $q_{Exh}$ ) and unaccounted losses ( $Q_{Other\ loss}$ ,  $q_{Other\ loss}$ ).

##### A. Comparison of engine performance

Fig. 4a and 4b show simulation results of  $N_e$  and  $g_e$  according to the load and speed. In Fig. 4a,  $N_e$  tends to increase when load or speed rising. However, the rate of augmentation in the load is greater than that in the speed. For the  $g_e$  shown in Fig 4b, the trend of  $g_e$  decreases when the load increases at different speed. At a steady load mode, the  $g_e$  reaches the lowest value in the speed ranges from 1400-1600 rpm.

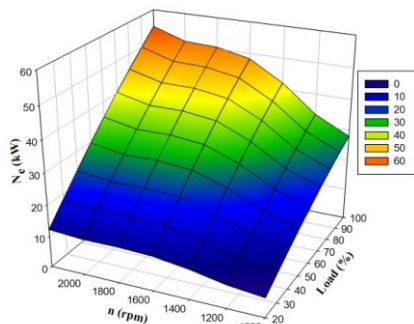


Fig.4a.  $N_e$  at the engine operating modes

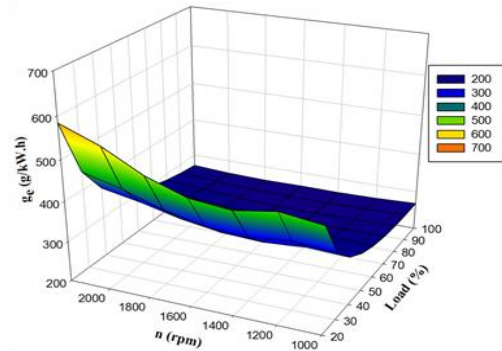


Fig.4B:  $g_e$  at the engine operating modes

##### B. The percentage of waste heat energy transfer to useful power

Energy supplied to an ICE engine comes from burning the fossil fuel. A part of this energy is transformed into useful power  $N_e$ . The amount of heat transferred to  $N_e$  ( $q_e$ ) is presented in Fig. 5. The results show that, as the load increases,  $q_e$  rises and reaches the maximum at full load about 29.5-32%. At each steady load mode, as the speed increases,  $q_e$  tends to reduce. This tendency due to increased mechanical losses directly proportional to the speed of engine.

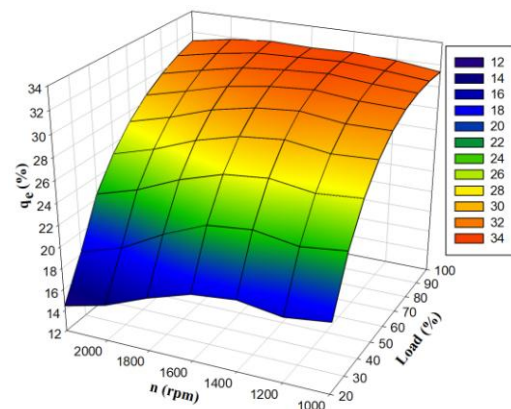


Fig.5 The ratio of heat transferred to useful power according to the engine modes

##### C. The ratio of heat losses to the coolant system

The two main parts of the heat waste are the heat carried away by the exhaust gases and transferred to the coolant system. Fig. 6a and 6b illustrate the amount and ratio of thermal energy transferred to the cooling water ( $Q_{Cool}$ ) at the engine operating modes. The results showed that  $Q_{Cool}$  increases directly proportional to load at different speeds. Similarly this heat rises when the speed increases.  $Q_{Cool}$  reaches the highest value in full load and rated speed. The heat transfer coefficient for cooling water ( $q_{Cool}$ ) varies between 23.5-36.5% as shown in Fig. 6.b and it tends to decrease when the speed increases. In an opposition, it rises proportional to load and reaches maximum at full load.

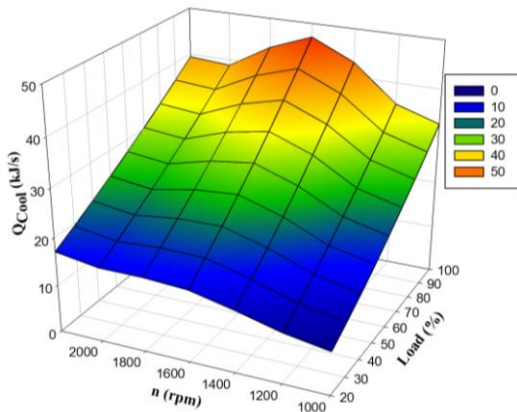


Fig.6a: The amount of heat losses to the coolant system according to engine modes

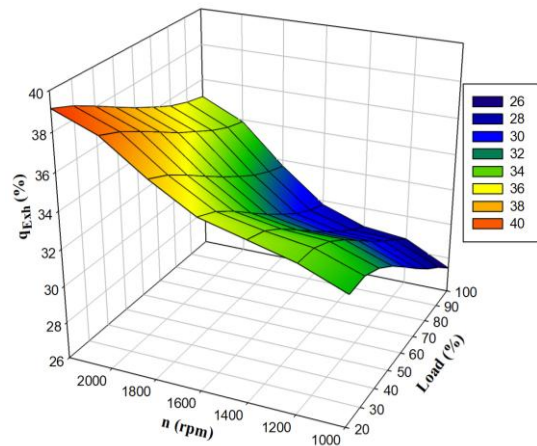


Fig.7b: The ratio of heat losses to exhaust gases according to the engine modes

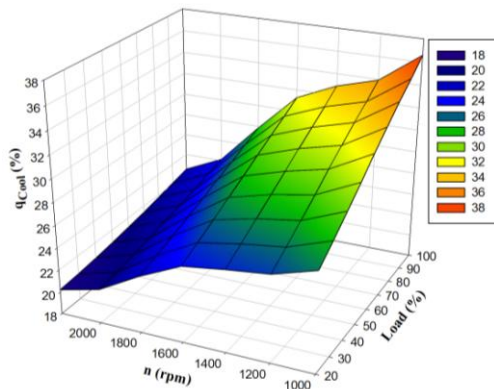


Fig.6b: The ratio of heat losses to the coolant system according to the engine modes

**C. Heat energy losses to exhaust gases**

Fig. 7a and 7b show the amount ( $Q_{Exh}$ ) and the ratio ( $q_{Exh}$ ) of heat which are carried away by exhaust gases in the engine's operating modes. The results show that  $Q_{Exh}$  increases proportional to load and speed, and reaches maximum at full load and rated speed. While,  $q_{Exh}$ , as shown in Fig. 7b, tends to inverse proportion to load and reaches the highest value at the rated speed with ranges from 27.5-38%.

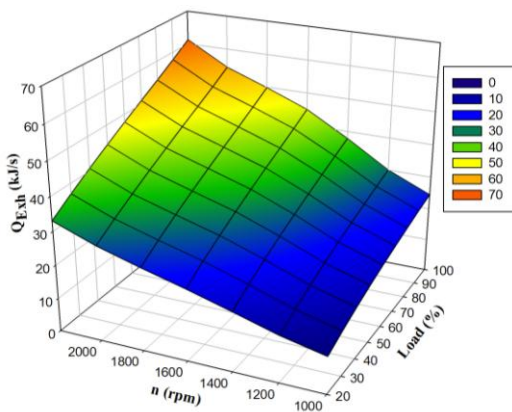


Fig.7a: Heat energy losses to exhaust gases according to the engine modes

**D. The unaccounted energy losses inside the engine**

According to heat balance of engine, the total energy generated by burning the fuel is divided into three main parts: heat transfers to useful power; losses to cooling water and exhaust gas; and other small thermal losses ( $Q_{Other\ loss}$ ) including mechanical losses (mostly), incomplete combustion of fuel, losses at intake and exhaust manifold, heat radiation, etc. shown in Fig. 8a and 8b. The rules of  $Q_{Other\ loss}$  shows that it is proportional to the speed and inversely proportional to the load (Fig. 8a).  $Q_{Other\ loss}$  reaches the maximum value at idle mode (because the large of unburn fuel) and rated speed (mechanical losses is the greatest). For this ratio of heat ( $q_{Other\ loss}$ ) as shown in Fig. 8b, the value varies widely from 4.5-43.5%, and tends to increase when the engine's speed rising or decrease when increasing the engine load. Consequently, it reaches the minimum value at the full load.

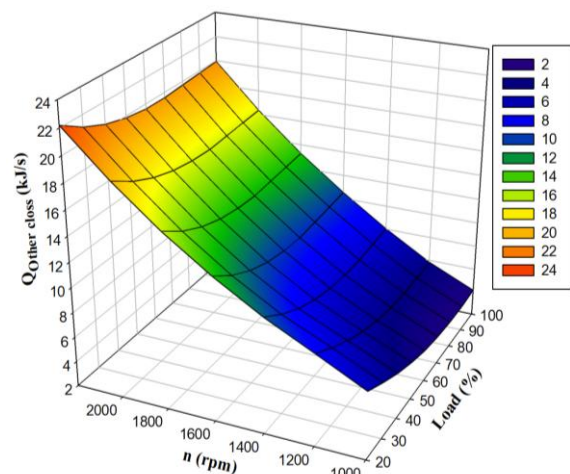
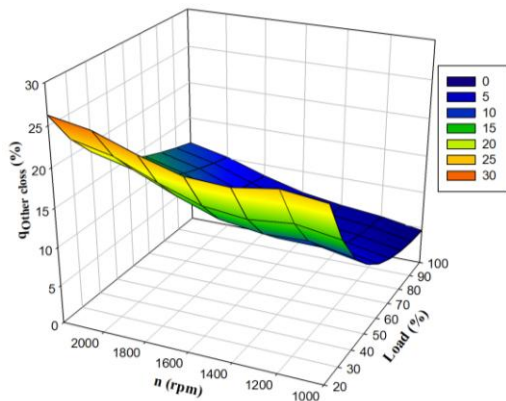


Fig.8a: The unaccounted energy losses inside the engine according to the engine modes



**Fig.8b: The ratio of unaccounted energy losses inside the engine according to the engine modes**

### V. CONCLUSION

The paper has successfully built up the simulation model of the D243 engine on AVL-Boost with the reliable that can be used to calculate the amount and ratio of heat energy transferred to useful power, lost to cooling water, exhaust gases and others. The results show that at full load and rated speed the heat  $q_e$  is about 29.5-32%;  $q_{Cool}$  is about 26% and reduces gradually as the speed down;  $q_{Exh}$  is about 32.5% while  $q_{Other loss}$  accounts for about 10% and they tend to decrease directly proportional to speed.

The results of this study will be very important factors to calculate, design and implement the system utilizes the unuseful energy transferred to cooling water and exhaust gas of the ICE engine.

### ACKNOWLEDGMENT

This work was supported by Ministry of Education and Training for the financial support under the grant contracts No.2017 BKA 39. This research was also assisted by ICE-Lab at Hanoi University of Science and Technology for the test equipment as well as AVL-Boost program.

### REFERENCES

- [1] Alberto Boretti, "Recovery of exhaust and coolant heat with R245fa organic Rankine cycles in a hybrid passenger car with a naturally aspirated gasoline engine," *Applied Thermal Engineering* 36 (2012), pp 73–77.
- [2] J. S. Jadhao and D. G. Thombare, "Review on Exhaust Gas Heat Recovery for I.C. Engine," *International Journal of Engineering and Innovative Technology*, Volume 2, Issue 12 (June 2013), pp 93-100.
- [3] B. Orr, A. Akbarzadeh, M. Mochizuki and R. Singh, "A review of car waste heat recovery systems utilizing thermoelectric generators and heat pipes," *Applied Thermal Engineering* 101 (2016), pp 490–495.
- [4] Giorgio Zamboni and Massimo Capobianco, "Influence of high and low pressure EGR and VGT control on in-cylinder pressure diagrams and rate of heat release in an automotive turbocharged diesel engine," *Applied Thermal Engineering* 51 (2013), pp 586-596.
- [5] Giorgio Zamboni, Simone Moggia and Massimo Capobianco, "Hybrid EGR and turbo charging systems control for low NO<sub>x</sub> and fuel consumption in an automotive diesel engine," *Applied Energy* 165 (2016), pp 839–848.
- [6] Kai Shen, Fangbo Li, Zhendong Zhang, Yuedong Sun and Congbo Yin, "Effects of LP and HP cooled EGR on performance and emissions in turbocharged GDI engine," *Applied Thermal Engineering* 125 (2017), pp 746–755.
- [7] Jiaqiang Ea, Dandan Hana, Yuanwang Denga, Wei Zuoa, Cheng Qian, Gang Wu, Qingguo Peng and Zhiqing Zhang, "Performance enhancement of a baffle-cut heat exchanger of exhaust gas recirculation," *Applied Thermal Engineering* 134 (2018), pp 86–94.
- [8] Pavlos Dimitriou and Taku Tsujimura, "A review of hydrogen as a compression ignition engine fuel," *International journal of hydrogen energy* 42 (2017), pp 24470-24486.
- [9] Siddesh Rao and Alhate Dipak, "Review of Hydrogen as a Fuel in IC Engines," *International Journal of Science and Research*, Volume 7, Issue 7 (July 2018), pp 914-922.
- [10] M. Hatami, D.D.Ganjiand M.Gorji-Bandpy, "Numerical study of finned type heat exchangers for ICEs exhaust waste heat recovery," *Case Studies in Thermal Engineering* 4 (2014), pp 53–64.
- [11] Mohsen Ghazikhani, Mohammad Hatami, Davood Domiri Ganji, Mofid Gorji-Bandpy, Ali Behravan and Gholamreza Shahi, "Exergy recovery from the exhaust cooling in a DI diesel engine for BSFC reduction purposes," *Energy* 65 (2014), pp 44-51.
- [12] E.H. Wang, H.G. Zhang, B.Y. Fan, M.G. Ouyang, Y. Zhao and Q.H. Mu, "Study of working fluid selection of organic Rankine cycle (ORC) for engine waste heat recovery," *Energy* 36 (2011), pp 3406-3418.
- [13] V. Pandiyarajan, M. Chinna Pandian, E. Malan, R. Velraj and R.V. Seeniraj, "Experimental investigation on heat recovery from diesel engine exhaust using finned shell and tube heat exchanger and thermal storage system," *Applied Energy* 88 (2011), pp 77–87.
- [14] R. Saidur, M. Rezaei, W.K. Muzammil, M.H. Hassan, S. Paria, M. Hasanuzzaman. Technologies to recover exhaust heat from internal combustion engines. *Renewable and Sustainable Energy Reviews* 16 (2012) 5649–5659.
- [15] Saiful Bari and Shekh N.Hossain, "Waste heat recovery from a diesel engine using shell and tube heat exchanger," *Applied Thermal Engineering*, Volume 61, Issue 2, (3 November 2013), pp 355-363.
- [16] FU Jian-qin, LIU Jing-ping, XU Zheng-xin, DENG Bang-lin and LIU Qi, "An approach for IC engine coolant energy recovery based on low-temperature organic Rankine cycle," *J. Cent. South Univ.* (2015) 22, pp 727–734. DOI: 10.1007/s11771-015-2576-9.
- [17] Tae Young Kim, Assmelash a. Nagash and Gyubaek Cho, "Waste heat recovery of a diesel engine using a thermoelectric generator equipped with customized thermoelectric modules," *Energy Conversion and Management* 124 (2016), pp 280-286.
- [18] Qimin Cao, Weiling Luan and Tongcai Wang, "Performance enhancement of heat pipes assisted thermoelectric generator for automobile exhaust heat recovery," *Applied Thermal Engineering* 130 (2018), pp 1472–1479.



ISSN: 2277-3754

ISO 9001:2008 Certified

International Journal of Engineering and Innovative Technology (IJET)

Volume 8, Issue 4, October 2018

- [19] Murat Emre Demir and Ibrahim Dincer, “Development and heat transfer analysis of a new heat recovery system with thermoelectric generator,” International Journal of Heat and Mass Transfer 108 (2017), pp 2002–2010.
- [20] Tae Young Kim, Assmelash Negash and Gyubaek Cho, “Experimental and numerical study of waste heat recovery characteristics of direct contact thermoelectric generator,” Energy Conversion and Management 140 (2017), pp 273–280.
- [21] AVL-List GmbH (2009), BOOST v.2009 Users Guide & Theory, Hans-List-Platz 1, A-8020 Graz, Austria.
- [22] Colin R. Ferguson and Allan T. Kirkpatrick (2001), Internal Combustion Engine: Applied Thermo science, Second edition, John Wiley & Sons, Inc.